Visakhapatnam Chapter

Proceedings of Indian Geotechnical Conference 2020
December 17-19, 2020, Andhra University, Visakhapatnam

Effect of Liquefaction on Behavior of Strip Footings on Sands in Roorkee

Mahendra Singh[1] and B.K. Maheshwari[2]

[1]Assistant Professor, Department of Civil Engineering, National Institute of Technology Hamirpur, Himachal Pradesh-177005. E-mail: manendra@nith.ac.in
[2]Professor, Department ofEarthquake Engineering, IIT Roorkee, Uttarakhand – 247667.
E-mail: bk.maheshwari@eq.iitr.ac.in

Abstract. Many strong earthquakes have shown the risk of constructing strip footings in areas where earthquake induced liquefaction is occurred. Liquefaction analysis of strip footings mainly depends on excess pore pressure, degraded bearing capacity, liquefaction induced settlement. This paper corresponds to liquefaction performance of strip footings. Analytically studies are carried for determining the effect of liquefaction on strip footings resting on sand. The evaluation of liquefaction potential was determined using standard penetration data of sand layers. Parametric studied have also been performed by varying relative density of soil, peak ground acceleration and location of liquefiable layer below the footing. It can be found that the liquefaction induced settlement is directly related to Peak Ground Acceleration. Bearing capacity does not greatly influenced by PGA because it is mainly directly related to excess pore pressure. The location of liquefiable layer below the footing affects the liquefaction performance, if depth below increases then there is decrease in dynamic settlement and increase in bearing capacity.

Keywords: Liquefaction; Strip Footings; Earthquake

1 Introduction

Effect of liquefaction on shallow foundations is very interesting topic for research point of view. Generally on liquefied soils, deep foundation is to be provided and lot of research works have been done on earthquake resistant design of deep foundation on liquefied soils. But in residential buildings, it is not advisable to provide deep foundation. So if any liquefaction susceptible site exists in residential area then shallow foundation is required.

Estimation of seismic response of shallow foundation during a strong earthquake has been proven a difficult task throughout the years. This is due to, that soil behaves in a highly non-linear manner when subjected to large cyclic strains. It can deform substantially and then, when saturated, may develop high pore pressures and finally liquefaction occurs in it. The soil strength may reduce under seismic loading depending on the type of soil and seismic motion. Due to earthquake, pore pressure builds up and undrained conditions may result in decrease in strength and an increase in settlement. Failures of shallow foundations by earthquake occur due to increase in settlement. However, bearing capacity failures have also been observed during Niigata earthquake (1964) in Japan and Izmit earthquake (1999) in Turkey. [1]

Liquefaction leads to severe loss of bearing capacity and increase settlements which lead to serious damage to the superstructures. Construction of shallow foundation upon the liquefiable soil is possible when a sufficient thick non-liquefiable soil crust (such as clay, dense sand, dry sand and improved soil), between the foundation and liquefiable soil, exists. In this paper, liquefaction performance of a strip footing is discussed considering various parameters such as PGA, relative density of soil medium and location of liquefiable soil below the footing.

2 Problem Definition

2.1 SPT data

Analysis is carried out assuming a strip footing of width 4 m. Depth of footing is 1.5 m below the ground surface. Water table is located at 4.5 m below the ground surface and Avg. load on the footing is assumed to be 100 kPa. The soil data for analysis was obtained from Department of Earthquake Engineering, IIT Roorkee. Table 1 shows unit weights and SPT (N) values for DEQ campus [2].

Table 1. Unit weights and N value of DEQ, IIT Roorkee [2]

Depth (m)	Dry unit weight, γ (kN/m^3)	Saturated unit weight, γ_{sat} (kN/m^3)	Uncorrected N value
1.5	14.5	-	5
3.0	14.5	-	11
4.5	-	16.93	5
6.0	-	16.18	8
7.5	-	15.46	8
9.0	-	17.89	11
10.0	-	17.85	12

2.2 Shear strength parameters of soil

From grain size distribution curves it can be observed that the soil type is sand at all depth. So cohesion of soil is zero for this site. Friction angle ϕ is calculated by SPT number N and unit weights. For this corrected N values are used. For correction of SPT

N value overburden pressure and dilatancy corrections are to be applied. Corrected N values are determined and shown in Table 2.

Table 2. Calculation of corrected N values

Depth (m)	N	σ_v' (kN/m^2)	C_N	N_1	N_2
1.5	5	21.75	1.5	7.5	7.5
3.0	11	43.5	1.28	14.08	14.08
4.5	5	68.895	1.12	5.6	5.6
6.0	8	78.165	1.08	8.64	8.64
7.5	8	86.355	1.05	8.4	8.4
9.0	11	98.19	1.0	11	11
10.0	12	106.04	0.98	11.76	11.76

Overburden correction factor is calculated from equation (1). [3]

$N_1 = C_N N_m$ (1a)

Where, $C_N = 0.77 \log_{10}\left(\frac{2000}{\sigma_v'}\right)$ (1b)

N_m is measured N value. σ_v' is the vertical effective stress in kN/m^2.
Dilatancy correction is calculated using Eq. (2). [4]

$N_2 = (N_1 + 15) / 2$ for $N_1 > 15$ (2a)

$N_2 = N_1$ for $N1 \le 15$ (2b)

Depth of influence below the footing level is taken as 2.1 times of width of footing. From Table 1, Avg. saturated unit weight below the footing calculated as 6.86 kN/m^3. From Table 2, Avg. corrected N value below the footing obtained as 10. From IS 6403:1981 [5], for corresponding corrected N value, friction angle from comes out as 30 deg.From above calculation, we summarized the problem and this is shown by Fig. 1.

2.3 Earthquake loading

Sinusoidal motion of earthquake was taken for the analysis. Since Roorkee city lies in Zone IV of the seismic zone of India therefore following earthquake properties were adopted for simulation.

Maximum peak ground acceleration, a_{max}= 0.24 g, Number of cycle N = 10, Time period= 0.4 sec.

Magnitude = 7.0

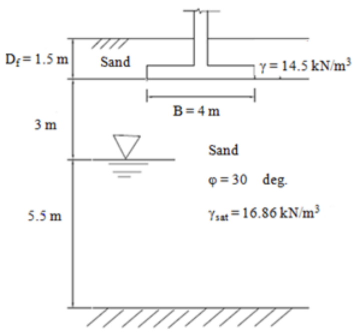

Fig. 1. Strip footing resting on sand layer.

3 Methodology

3.1 Static bearing capacity, settlement and liquefaction potential

Static bearing capacity is determined as per IS 6403:1981 [5]. For sandy soil static settlement is calculated using IS 8009 (Part1): 1976 [6]. Liquefaction potential is calculated by the method given by Seed and Idriss (1971) [7].

3.2 Dynamic bearing capacity and settlement due to liquefaction

Analysis consists of three steps: a) evaluation of excess pore pressure, b) dynamic bearing capacity and c) dynamic settlement.

Evaluation of excess pore pressure. A parameter i.e. excess pore pressure (EPP) ratio is defined which is represented for the entire sand layer. Since excess pore pressure ratio developing in the region under the footing remain less than the EPP ratio under the free field. It has been taken in consideration that an active failure zone forms under the footing, forcing the soil in the free field into passive failure. Following this logic, a weighted average of the excess pore pressure ratios underneath the footing (r_{foot}) and in the free field (r_{ff}) was taken for the analytical solution. For strip footing, average excess pore pressure is calculated as $r_u = (r_{foot} + r_{ff})/2$. [8, 9]
Excess pore pressure in free field condition ($\Delta u_{ff,\,c}$) and under the footing ($\Delta u_{footing,\,c}$) due to earthquake are calculated by finite element method using Cyclic 1D software and Cyclic TP Software [10]. EPP for both cases is calculated at characteristic point which lies at a certain depth below the centre line of footing. This depth is calculated from Eq. 3. [8, 9]

$$Z_c = H + \left[1.0 - 0.5\left(\frac{B}{L}\right)^3\right]B \tag{3}$$

For strip footing Z_c= H+B. Where, H is thickness of non-liquefiable layer, B is width of footing and L is the length of footing. Further, $\Delta u_{foot,c}$ is EPP under the footing and $\Delta u_{ff,c}$ is the EPP under the free field at characteristic depth. The $\Delta\sigma_{v,\,c}$ is the additional vertical stress imposed to the characteristic point by the foundation load and $\sigma'_{v,c}$ is the geostatic vertical effective stress. [9]
Subsequently EPP ratio under the footing (r_{foot}) and free field (r_{ff}) are calculated from Eqs. 4 and 5, respectively. [9]

$$r_{foot} = \frac{\Delta u_{foot,c}}{\sigma'_{v,c} + \Delta\sigma_{v,c}} \tag{4}$$

$$r_{ff} = \Delta u_{ff,c} / \sigma_{vc}' \tag{5}$$

Dynamic Bearing Capacity. A simple failure mechanism which may be used to calculate the degraded bearing capacity of shallow foundations at the end of shaking, while the soil below the soil crust is still in a liquefied state, is shown in Fig. 2. The footing punches through the crust forcing the development of a wedge-type failure mechanism within the liquefied subsoil. [11]

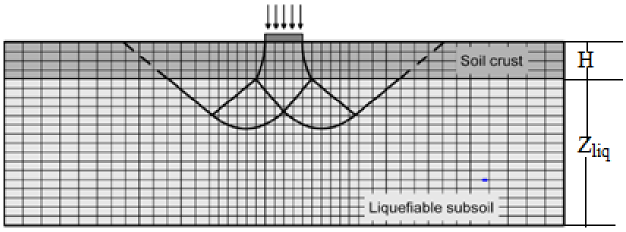

Fig. 2. Composite mechanism for end-of-shaking failure of shallow foundations resting on a soil crust over liquefied subsoil [11].

In the failure mechanism of Fig. 2, it is assumed that the shear strength of the liquefied soil is expressed in terms of a degraded friction angle ϕ_d and it is calculated from Eq. 6. [11]

$$\tan\phi_d = (1 - r_u)\tan\phi \qquad (6)$$

Where ϕ is the actual friction angle of the sand and r_u is the excess pore pressure ratio induced by ground shaking, taken as uniform over the entire liquefied layer. From Eq. 6, increase in pore pressure ratio leads to decrease in friction angle. Therefore, excess pore pressure ratio is most important parameter for liquefaction analysis. Ultimate degraded bearing capacity of strip footing is given by Eq. 7. [11]

$$(q_u)_{deg} = \gamma_1'(D_f + H)N_{q2} + 0.5\gamma_2'BN_{\gamma2} + (\gamma_1'H^2/B)(1 + 2D_f/H)K_s\tan\phi_1 - \gamma_1'H \qquad (7)$$

Bearing capacity degradation factor is determined from Eq. 8. [11]

$$\zeta = (q_u)_{deg} / q_u \qquad \leq 1 \qquad (8)$$

Where, H is thickness of non-liquefiable sand layer, D_f is the depth of foundation below the ground surface, N_{q2} and $N_{\gamma2}$ are the bearing capacity factors of the liquefied layer for the degraded friction angle ϕ_d, γ_1' is submerged unit weight of non-liquefiable sand layer, γ_2' is submerged unit weight of liquefied layer, ϕ_1 is friction angle for non-liquefiable sand layer, K_s is coefficient of punching shear resistance on the vertical plane through the footing edges. K_s is determined from Fig. 4. K_s depend on approximate bearing capacity ratio which is determined from Eq. 9. [12]

$$q_2 / q_1 = (\gamma_2 N_{\gamma 2} / \gamma_1 N_{\gamma 1}) \qquad (9)$$

If H =0 i.e. footing is directly on liquefiable sand then Eq. 7 can be written as:

$$(q_u)_{deg} = \gamma_1' D_f N_{q2} + 0.5\gamma_2' B N_{\gamma 2} \qquad (10)$$

Dynamic Settlement. Dynamic settlement is calculated from Eq. 11. [13]

$$S_{dyn} = c a_{\max} T^2 N \left(\frac{Z_{liq}}{B} \right)^{1.5} \left(\frac{1}{FS_{\deg}} \right)^3 \qquad (11)$$

Coefficient c is equal to 0.008 and 0.035 for square and strip foundations, respectively. Here a_{max} is seismic peak ground acceleration, T is predominant excitation time period, N is number of cycles corresponding to PGA (a_{max}), Z_{liq} is the thickness of liquefiable layer, B is width of foundation, q is average footing load. [13]

4 Results and Discussions

4.1 Static bearing capacity and settlement

Static ultimate bearing capacity strip footing shown in Fig. 1 was found to be 481.16 kN/m^2 whereas settlement of footing was 40.91 mm.

4.2 Evaluation of liquefaction potential

Liquefaction potential was calculated by the method given by Seed and Idriss (1971) [7]. Figure 3 shows the variation of cyclic stress ratio with the depth. It can be seen from Fig. 3a that cyclic stress ratio of earthquake excitation (CSR) was found to be greater than the cyclic resistance ratio of soil (CRR) for all the depth below the water table. From Fig. 3b it can be seen that factor of safety against the liquefaction was found to be less than unity. Therefore soil below the water table is susceptible to liquefy under the earthquake loading.

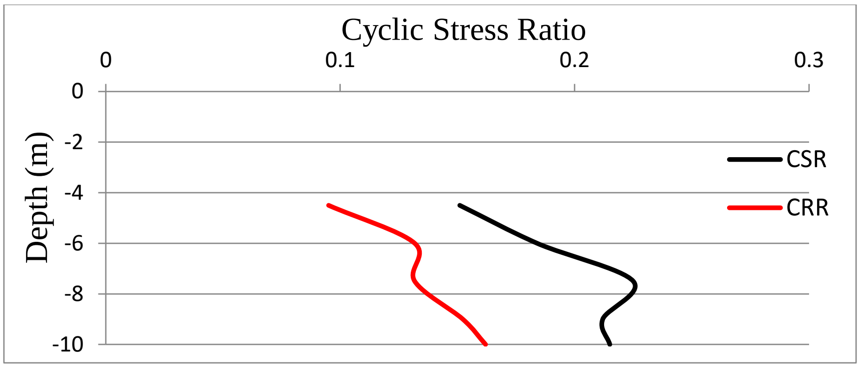

Fig. 3a. Evaluation of liquefaction potential for sand

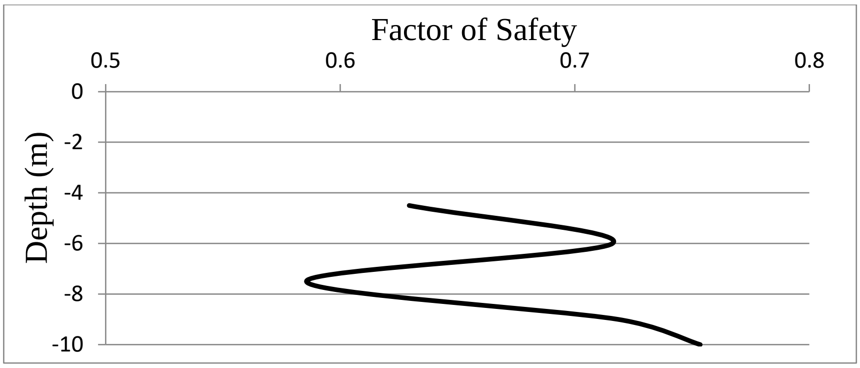

Fig. 3b. Factor of safety against the liquefaction

4.3 Excess pore pressure

Excess pore pressure ratio under the footing is measured at characteristic depth and given by equation (12). [9]

$$r_{foot} = \frac{A}{1 + \Delta\sigma_{v,c} / \sigma'_{v,c}} \qquad (12)$$

Where, $\Delta\sigma_{v,c}$ is the additional vertical stress imposed to the characteristic point by the foundation load and $\sigma'_{v,c}$ is the geostatic vertical effective stress. $\Delta u_{ff,c}$ is excess pore pressure at characteristic depth under the free field condition. Subsoil dilation effect may be conservatively overlooked, assuming a correction factor A= 1.

For free field excess pore pressure ratio is assumed to unity at charecterstic depth. Characteristic depth (Z_c = H + B) is calculated as 7 m below the footing. Subsequently effective stress at this characteristic point was calculated as 94.245kN/m^2.

Avg. excess pore pressure ratio $r_u = (r_{foot} + r_{ff})/2 = 0.74$

4.4 Dynamic bearing capacity and dynamic settlement

Following values are obtained by the methods as discussed in section 3.2.2 and 3.2.3.

Degraded bearing capacity q_{ultd} = 172.97kN/m^2

Degradation factor ζ = 0.36

Dynamic settlement S_{dyn} = 40.34 mm.

Total settlement S =81.25mm

Effect of liquefaction is summarized in Table 3. It can be observed from Table 3 that bearing capacity was found to reduce 36% due to liquefaction as compared to static condition whereas total settlement has increased almost two times as compared to static condition

Table 3. Effect of liquefaction

	Static condition	Dynamic condition
Ultimate bearing capacity (kN/m$^{2)}$	481.16	172.97
Settlement (mm)	40.91	81.25

5 Parametric studies

5. 1 Effects of relative density of sand

In this section strip footing of width 5m is taken. Depth of footing is 1m below the ground surface. Water table is assumed to be located at the ground surface. Two cases are taken for the soil properties:

Case 1: Footing is resting on loose sand

Case 2: Footing is resting on medium sand

Properties of soils are given below in Table 4: N is determined from Seed and Idriss (1971) formula by equation 13. [7]

$$V_s = 61.4\ N^{0.5} \qquad (13)$$

Table 4. Properties of Sand

Type of soils	Shear wave velocity V_s(m/s)	N	Friction angle ϕ (degrees)	Unit weight γ_{sat} (kN/m^3)
Loose sand	185	9	29	17
Medium sand	205	11	31.5	19

For both the cases Poisson's ratio (0.4) and coefficient of permeability are the same (6.6×10^{-5} m/sec). Average load on footing for both cases is 125 kPa. Effects of liquefaction are found out for both cases. Figure 4 describe the above problem.

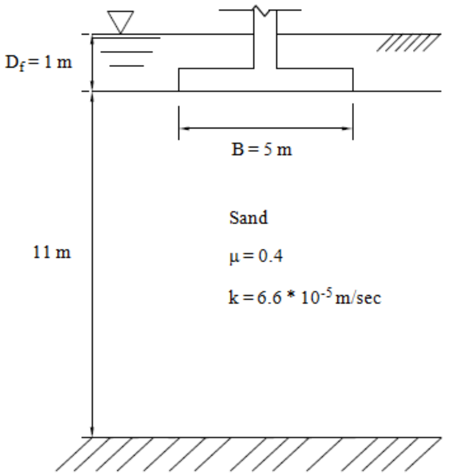

Fig. 4. Problem diagram of a footing resting on loose or medium sand.

Static Bearing capacity and static settlement are calculated as per IS 6403:1981 [5] and IS 8009:1976 [6] respectively and shown in Table 5.

Table 5. Calculations of Bearing Capacity and settlement

Type of soil	q_{ult} (kN/m^2)	Settlement (mm)
Loose sand	200.47	165
Medium sand	459.79	82.5

Evaluation of liquefaction potential. Factor of safety against the liquefaction has been determined as discussed in section 3.1 and it has been shown in Fig. 5. From Fig. 5, it can be observed that liquefaction occurs at all depths for both loose and medium sand.

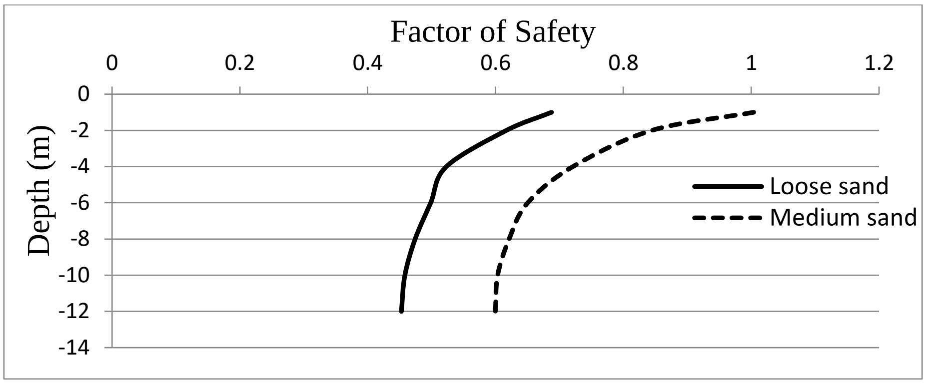

Fig. 5. Factor of safety against liquefaction for loose and medium sand.

Excess pore pressure

Under the Free Field. EPP is determined from CYCLIC 1D software. CYCLIC 1D is a nonlinear finite element program for execution of one dimensional site amplification and liquefaction simulation. Following properties were taken for analysis:
a_{max} = 0.2 g, T = 0.25 sec, N = 10 or f = 4 Hz.
Rayleigh Damping parameters: A_m = 0.215423, A_k = 0.0009094557

Under the Footing. EPP under the footing is determined by CYCLIC TP software by nonlinear analysis. CYCLIC TP is a finite element program for two dimensional (2D) analysis of shallow foundations, under liquefaction-induced seismic excitation scenarios. Following footing parameters were adopted for analysis:
B = 5 m, D_f = 1 m, Ht. above the G.S. = 1m, E_s = 25 GPa, μ = 0.25, Mass density = 2500 kg/m^3
Excess pore pressure calculated from softwares CYCLIC 1D & CYCLIC TP is shown in Figures 6 and 7 for loose sand and medium sand respectively. Similarly EPP ratio for both cases has been shown in Figs. 8 and 9.

From Figures 6 and 7 it is shown that epp under the free field is less than the epp under the footing but from Figures 8 and 9 it is shown that epp ratio is quite high under the free field than the under the footing. Characteristic depth (Z_c) is 6 m below the ground level. Avg. EPP ratio is calculated at this depth and given in Table 6.

Table 6. EPP Ratio for loose and medium sand

Type of soil	r_{ff}	r_{foot}	r_u
Loose sand	0.98	0.25	0.615
Medium sand	0.87	0.31	0.59

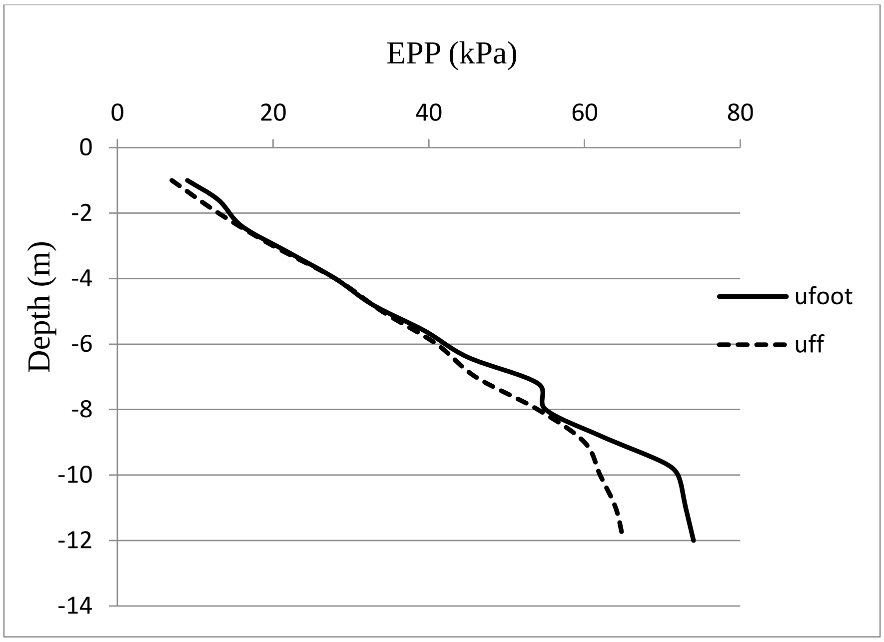

Fig. 6. Excess Pore Pressure for loose sand.

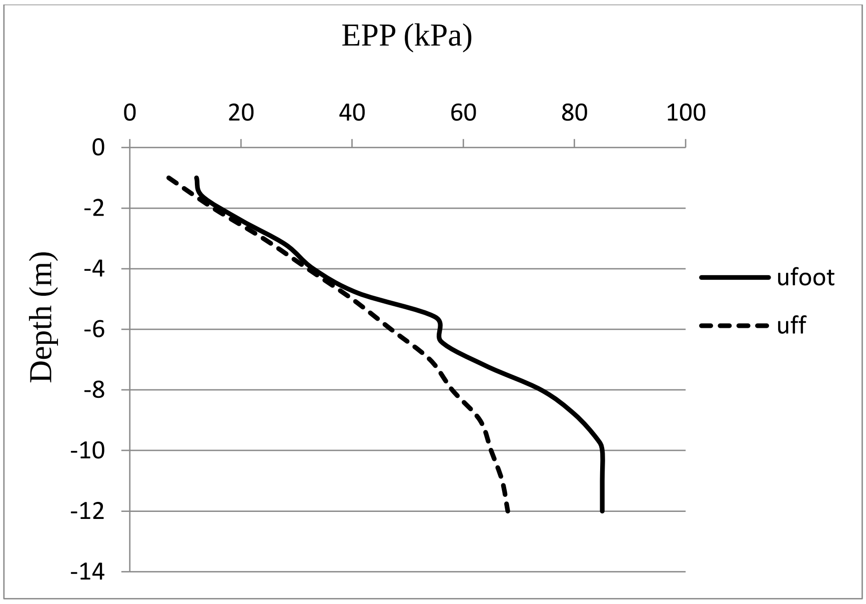

Fig.7. Excess Pore Pressure for medium sand.

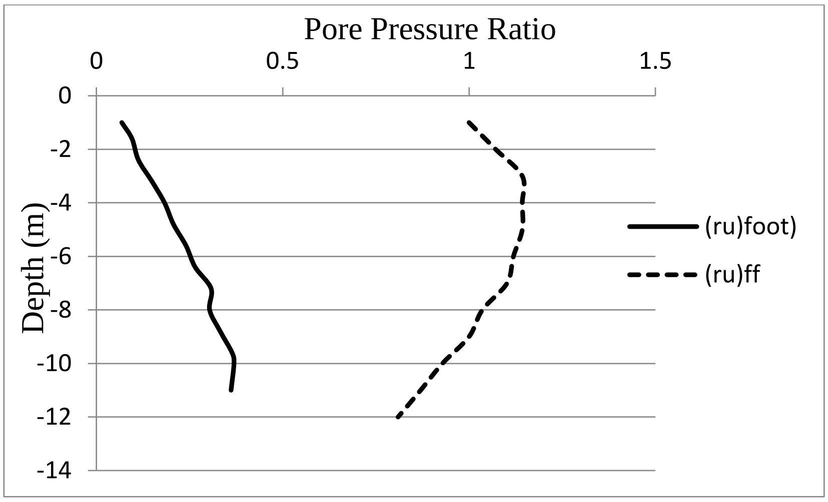

Fig. 8. EPP Ratio for loose sand.

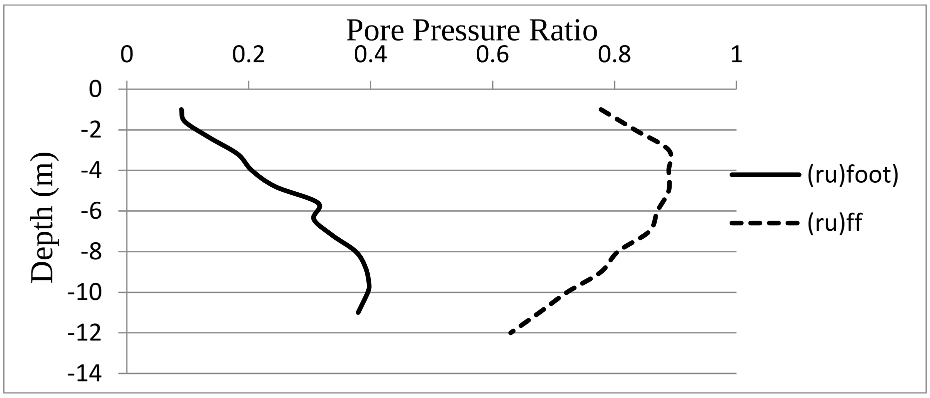

Fig. 9. EPP Ratio for medium sand.

Dynamic bearing capacity and settlement. Calculated Degraded bearing capacity and dynamic settlement are shown in Table 7. .

Table 7. Analysis with seismic forces for loose and medium sand

Type of soil	r_u	ϕ_d (deg.)	q_{ultd} (kN/m^2)	FS_{deg}	S_{dyn}(2)
Loose sand	0.615	12.05	56.96	0.456	1.5 m
Medium sand	0.59	14.10	87.55	0.70	41.55 cm

Effects of liquefaction are shown in Table 8.

Table 8. Effects of liquefaction for loose and medium sand

Type of soil	q_{ult} (kN/m^2)	q_{ultd} (kN/m^2)	ζ	S_{static}	S_{dyn}	Total S
Loose sand	200.47	56.96	0.28	165 mm	1.5 m	1.66 m
Medium sand	459.79	87.55	0.19	82.5 mm	45.69 cm	53.94 cm

It can be observed from Table 8, that effect of liquefaction is significantly greater for loose sand as compared to medium sand.

5.2 Varying maximum acceleration

Peak ground acceleration (PGA) is the most important parameter for liquefaction. In this section effect of PGA on liquefaction is discussed. There is a footing of width 4m, resting on sand layer. The properties of footing and sand layer are shown in Fig. 10. Water table is located at the footing level. And depth of footing is 1m below the ground surface. In this section, parametric studies are carried out by varying PGA (a_{max}) and all other properties are kept constant.
Input motion: a_{max} is varying, T = 0.25 sec, N = 10
Footing properties: E_s = 25 GPa, μ = 0.25, Mass density = 2500 kg/m^3
Load on footing = 100 kPa
Figure 11 shows the liquefaction analysis for different PGA. Liquefaction does not occur for PGA 0.1g, but it occurs below the depth 2m from the footing for PGA 0.2g and at all depth below the footing for PGA 0.5g and 1g.

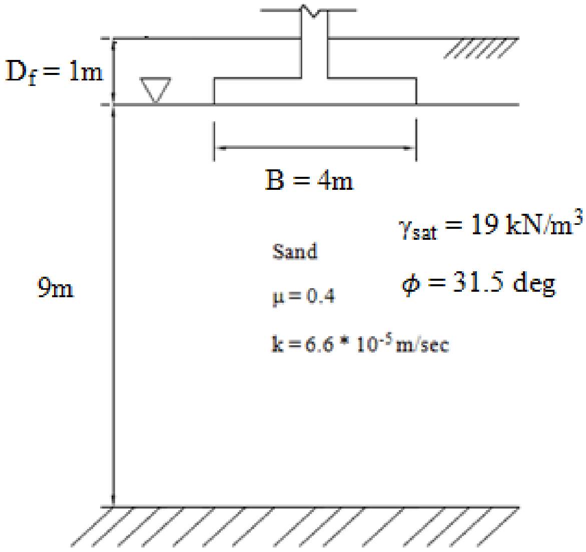

Fig.10. Strip footing on sand for different PGA.

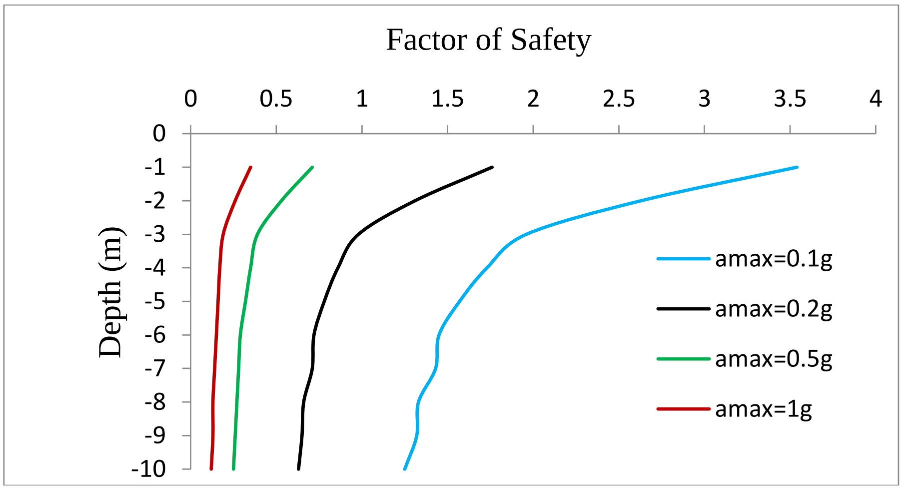

Fig. 11. Factor of safety against liquefaction for different PGA.

For analysis with seismic forces, same procedure is used as in section 5.1, then following values are obtained as shown in Table 9.

Table 9. Effects of PGA

a_{max}	r_u	ϕ (deg.)	q_u (kN/m^2)	ζ	S_{static}	S_{dyn} (mm)	Total S(mm)
0.1g	-	31.5	518.70	-	71.6	-	71.6
0.2g	0.55	15.4	167.54	0.25	71.6	41.19	112.79
0.5g	0.56	15.09	126.19	0.24	71.6	149.67	221.27
1g	0.57	14.76	121.53	0.23	71.6	233.08	304.68

For PGA 0.1g, there is no liquefaction. Table 9 shows that increase in PGA, settlement increases drastically and increase in PGA also leads to result in reduction in bearing capacity.

5.3 Varying the location of liquefiable layer

Shallow foundation cannot be constructed directly on liquefiable soil. Thickness of unliquefiable layer play a significant role in this case. In this section the role of this layer explained by taking various depth of liquefiable layer**.**

There is a footing of width 3m resting in soil. Water table is located at ground surface. Depth of footing is 1m below ground surface. Other properties are shown in Fig. 12.

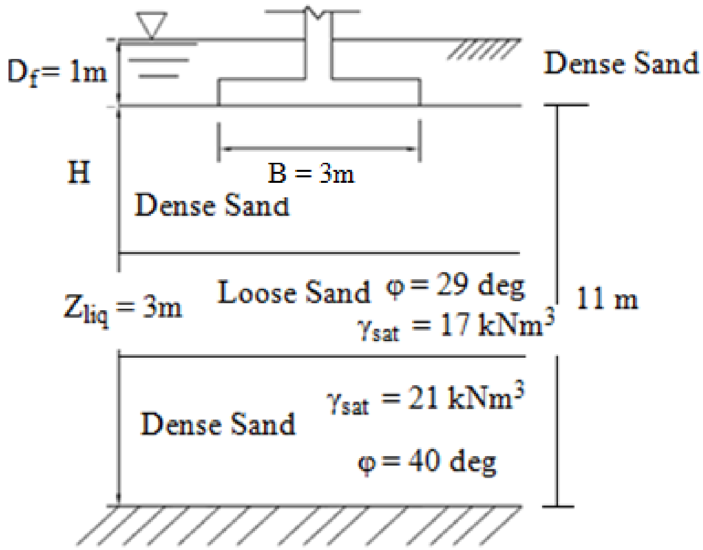

Fig. 12. Strip footing resting for different location of liquefiable sand.

Input motion: a_{max} = 0.4g, T = 1 sec of f = 1 Hz, N = 10
Footing properties: E_s = 25 GPa, μ = 0.25, Mass density = 2500 kg/m^3
Load on footing = 75 kPa
Thickness of liquefiable layer Z_{liq} = 3m
Same methodology used as explained in section 5.1**.**

Table 10. Effect of location of liquefiable layer

case	r_u	ϕ_d (deg)	q_{ultd} (kPa)	FS_{deg}	S_{dyn} (mm)
H=2m	0.45	16.96	222.76	2.96	53.43
H=4m	0.48	16.07	375.68	5.0	11.14
H=6m	0.58	14.4	499.18	6.6	4.85

It can be observed from Table 10, that change in location of unliquefiable layer has affected the excess pore pressure ratio. Friction angle decrease as increase in H, but there is decrease in coefficient of punching shear. Therefore increase in H result in increase in bearing capacity and factor of safety and also decrease the dynamic settlement. So increase in thickness of unliquefiable layer, reduces the effects of liquefaction.

6 Conclusions

Based on work, following conclusions are summarized

1. Liquefaction induced settlement and degraded bearing capacity are affected by type of soil, dimension of foundation and seismic excitation parameters.

2. When PGA increases, there is drastic increase in dynamic settlement but bearing capacity first increases after that marginally affected by PGA. This is because that dynamic settlement is directly related to PGA. Bearing capacity does not greatly influenced by PGA because it is mainly directly related to excess pore pressure.
3. The location of liquefiable layer below the footing affects the liquefaction performance, if depth below increases then there is decrease in dynamic settlement and increase in bearing capacity.

References

1. Day, R. W.: Geotechnical Earthquake Engineering Hand Book. McGraw Hill (2002).
2. Datta, M.K., Kamble, S., et.al.: Project report on Liquefaction Potential of DEQ Campus using SPT and Design of Pile Foundation, Department of Earthquake Engineering, IIT Roorkee, India (2006).
3. Peck, R. B., Hanson, W. E., Thornburn, T. H.: Foundation Engineering. Wiley, New York (1974).
4. Terzaghi, K., Peck, R.B.: Soil Mechanics Engineering practic. John Wiley & Sons, New York (1967).
5. Indian Standard (IS) 6403: Code of Practice for Determination of Bearing Capacity of Shallow foundation, Bureau of Indian Standards (1981).
6. Indian Standard (IS) 8009-Part I: Code of Practice for calculation of Settlements of foundation", Bureau of Indian Standards, New Delhi, (1976).
7. Seed, H.B., Idriss, I.M.: Simplified Procedure for Evaluating Soil Liquefaction Potential. Journal of Geotechnical Engineering Division, ASCE 97(9), 1249-1273 (1971).
8. Karamitors, D.K., Bouckovalas, G.D., Chaloulos, Y.K. Andrianopoulos, K.I.: Numerical analysis of liquefaction-induced bearing capacity degradation of shallow foundations on a two-layered soil profile. Soil Dynamics and Earthquake Engineering 44, 90–101 (2012).
9. Karamitors, D.K., Bouckovalas, G.D., Chaloulos, Y.K.: Insight into the Seismic Performance of Shallow Foundations. Journal of Geotechnical Geoenvironmental Engineering, ASCE 194(4), 599-607 (2013).
10. Cyclic 1 D and Cyclic TP: Softwares for ground response analysis and seismic analysis of shallow foundation. Version 1.2.
11. Bouckovalas, G., Dakoulas, P.: Liquefaction performance of Shallow Foundations in peresence of a Clay Crust, , Earthquake Geotechnical Engineering, Springer 6, 245–276 (2007).
12. Meyerhof, G.G., Hanna, A.M.: Ultimate bearing capacity of foundations on layered soils under inclined load. Canadian Geotechnical Journal 15(4), 565-572 (1978).
13. Karamitors, D.K., Bouckovalas, G.D., Chaloulos, Y.K. Seismic settlements of shallow foundations on liquefiable soil with a clay crust. Soil Dynamics and Earthquake Engineering 46, 64-76 (2013).